Distributed Cooperative Guidance for Simultaneous Missile Strike into a Polytopic Target Region

Burak Yücel[1] and Veysel Gazi[2]

***Abstract*—This study introduces a distributed cooperative guidance strategy enabling a swarm of missiles—modeled with detailed six-degree-of-freedom (6-DOF) dynamics—to execute a coordinated strike on a specified 2D polygonal zone embedded in 3D space. By integrating repulsion-attraction-based formation control with Proportional Navigation Guidance (PNG), the proposed method ensures collision-free trajectories and accurate terminal alignment. A key feature of the framework is its adaptive targeting region mechanism, which facilitates synchronized arrivals by aligning the swarm's geometry with the structure of the polytopic area. Simulations confirm that the approach maintains safety and precision under realistic 3D operational conditions.**

***Index Terms*—Cooperative guidance, missile swarm, simultaneous strike, collision avoidance, polytopic target region, 6-DOF nonlinear dynamics.**

I. Introduction

As modern defense environments grow increasingly sophisticated, the deployment of autonomous and networked weapon platforms has become a strategic priority. In particular, coordinated missile swarms have gained significant attention due to their potential to saturate enemy defenses, adapt to uncertain mission scenarios, and achieve mission objectives more reliably than conventional single-missile solutions [1]–[3]. Cooperative behaviors enable missiles to share information and adjust trajectories to ensure simultaneous arrival, enhancing effectiveness.

A key objective in cooperative missile guidance is to control the impact time with high precision. Early research on Impact-Time Control Guidance (ITCG) demonstrated the feasibility of forcing a missile to arrive at a target at a specified time, thereby minimizing the defender's opportunity to respond [4]. Recent advances in ITCG have integrated additional constraints, such as bounded missile speed and the ability to handle maneuvering targets or complex terminal conditions [1], [5]. By systematically managing each missile's arrival time, the swarm can engage the target in a tightly coordinated salvo attack, overwhelming defense systems and reducing the probability of interception.

Beyond time synchronization, modern mission requirements often demand multi-dimensional constraints that include formation shaping, collision avoidance, and spatial distribution of the swarm. Formation control is critical for enhancing interception probability and system robustness, as well-organized missile formations can improve stealth, enhance radar evasion, and ensure flexible engagement geometries [6]. For instance, behavior-based and leader-follower strategies have been employed to achieve desired formations [2], [3], while close-formation approaches enable missiles to reduce their radar cross-sections against maritime targets [7]. More advanced frameworks have explored three-dimensional cooperative guidance laws to achieve simultaneous attacks with impact-angle or trajectory constraints [8], [9], as well as fixed-time convergence methods that guarantee rapid and stable formation under uncertain conditions [10], [11].

The enforcement of collision-free trajectories further complicates the cooperative guidance problem. With multiple missiles maneuvering in proximity, ensuring safety margins is paramount. Methods for collision avoidance often leverage artificial potential fields, distributed consensus, and multi-agent optimization techniques [12]. Moreover, handling complex mission scenarios, including maneuvering targets and three-dimensional (3D) constraints, calls for advanced control strategies that can adapt in real-time [5], [13], robustly deal with communication and modeling uncertainties [14].

Realistic dynamic modeling constitutes another crucial aspect of modern missile swarm research. Simplified kinematic or planar assumptions may fail to capture the complex aerodynamic effects and rotational dynamics of high-speed interceptors. Increased model fidelity allows the development of more reliable guidance laws, leading to improved performance in highly dynamic and uncertain theaters. Studies on proportional navigation guidance (PNG), trajectory optimization, and advanced nonlinear control laws have paved the way for integrated solutions that are both practically implementable and theoretically sound [15], [16].

In this work, we present a novel cooperative guidance framework that integrates time synchronization, formation control, collision avoidance, and high-fidelity dynamics into a unified solution. We consider multiple surface-to-air, highly maneuverable missiles modeled with six-degrees-of-freedom (6-DOF) nonlinear dynamics to capture realistic behaviors. Unlike traditional leader-follower approaches, our fully distributed control enables each missile to make decentralized decisions using local and shared information. This ensures a stable, collision-free formation within a specified two-dimensional polytopic region, achieving simultaneous target arrival while accommodating varying mission parameters. By leveraging ITCG principles and consensus-based algorithms, this framework addresses key gaps in the literature.

The remainder of this paper is organized as follows: Section

[1] B. Yücel was a graduate student in the Graduate Program of Avionics Engineering, Yıldız Technical University, Istanbul, Turkey. burak.yucel1@std.yildiz.edu.tr

[2]V. Gazi is with the Department of Control and Automation Engineering, Yıldız Technical University, Istanbul, Turkey. vgazi@yildiz.edu.tr

II introduces the Problem Formulation and System Modeling. Section III details the Proposed Cooperative Guidance Framework. Section IV presents a Lyapunov Stability Analysis. Section V provides simulation results under realistic operational conditions. Finally, Section VI concludes the paper and suggests directions for future research.

Notation: Throughout the paper, superscripts (i), e, and b denote the i-th missile, the Earth-fixed frame, and the body frame, respectively. Vectors are in bold. All mathematical symbols are defined upon their first appearance for clarity.

II. Problem Formulation and System Modeling

A. Problem Formulation

We represent a swarm of N missiles as an undirected graph $\mathcal{G} = (\mathcal{V}, \mathcal{E})$, where $\mathcal{V} = \{1, \ldots, N\}$ and $\mathcal{E}$ captures pairwise communication links [17]. For any node i, the neighborhood $\mathcal{N}_i$ includes all nodes j for which information can be exchanged bi-directionally. We assume the graph is connected to ensure global consensus can be reached.

Let

$$\mathbf{p}_m^{e,(i)} = [x_m^{e,(i)}, y_m^{e,(i)}, z_m^{e,(i)}]^T \quad \text{and}$$

$$\mathbf{v}_m^{e,(i)} = [v_{m,x}^{e,(i)}, v_{m,y}^{e,(i)}, v_{m,z}^{e,(i)}]^T$$

be the position and velocity of the i-th missile in the inertial (Earth) frame. The objective is to direct each missile into a specified two-dimensional polytopic region $\mathcal{P} \subset \mathbb{R}^3$, defined by

$$\mathcal{P} = \Big\{ \mathbf{x} \in \mathbb{R}^3 \;\Big|\; \mathbf{n}^\top \mathbf{x} = d, \;\; A\,\mathbf{x} \leq \mathbf{b} \Big\}, \tag{1}$$

where $\mathbf{n}$ is the plane's normal vector, d positions the plane in space, and $(A, \mathbf{b})$ imposes polygonal bounds. We further assume an effective target location $\mathbf{p}_t^e \in \mathcal{P}$. The challenge is to orchestrate the swarm so that all missiles arrive at $\mathcal{P}$ with minimal time mismatch:

$$\lim_{t \to t_f} \Big([\mathbf{p}_m^{e,(i)}(t) - \mathbf{p}_m^{e,(j)}(t) - \mathbf{p}_t^e]^T \mathbf{r}_{ref} \Big) < \epsilon, \quad \forall\, i, j \in \mathcal{V}, \tag{2}$$

with ϵ a small bound and $\mathbf{r}_{ref} = \frac{\mathbf{a}}{\|\mathbf{a}\|}$ representing the normal direction to $\mathcal{P}$. Equivalently, all missiles should cross the target region's boundary at approximately the same moment t_f.

B. 6-DOF Nonlinear Missile Dynamics

A missile's 6-DOF model captures translational and rotational behavior more accurately than simpler point-mass assumptions [18]. For missile i,

$$m \dot{\mathbf{v}}_m^{b,(i)} = \mathbf{F}_{\text{aero}}^{b,(i)}(\cdot) + m\,\mathbf{g}^b + \mathbf{F}_T^{b,(i)}, \tag{3}$$

$$\mathbf{J}\,\dot{\boldsymbol{\omega}}^{b,(i)} = \mathbf{M}_{\text{aero}}^{b,(i)}(\cdot), \tag{4}$$

where $\mathbf{v}_m^{b,(i)}$, $\boldsymbol{\omega}^{b,(i)}$ are velocity and angular velocity in the body frame, $\mathbf{g}^b$ is gravity in the body frame, and m is the mass. The thrust $\mathbf{F}_T^{b,(i)}$ aligns with the missile's longitudinal axis and is derived from the commanded longitudinal acceleration $a_x^{b,(i)}$.

$$\mathbf{F}_T^{b,(i)} = \begin{bmatrix} m a_x^{b,(i)} \\ 0 \\ 0 \end{bmatrix}. \tag{5}$$

Aerodynamic forces and moments, $\mathbf{F}_{\text{aero}}^{b,(i)}$ and $\mathbf{M}_{\text{aero}}^{b,(i)}$, depend on the control surface deflections $\delta^{b,(i)}$, which are functions of lateral/vertical acceleration commands $a_y^{b,(i)}, a_z^{b,(i)}$.

$$\mathbf{F}_{\text{aero}}^{b,(i)} = f_{\text{aero}} \left(a_y^{b,(i)}, a_z^{b,(i)}, \mathbf{v}_m^{b,(i)}, \alpha^{b,(i)}, \beta^{b,(i)} \right), \tag{6}$$

$$\mathbf{M}_{\text{aero}}^{b,(i)} = f_{\text{moment}} \left(a_y^{b,(i)}, a_z^{b,(i)}, \mathbf{v}_m^{b,(i)}, \alpha^{b,(i)}, \beta^{b,(i)} \right). \tag{7}$$

We assume roll angle is actively regulated to zero. Thus, the control commands $(a_x^{b,(i)}, a_y^{b,(i)}, a_z^{b,(i)})$ map into realistic aerodynamic and thrust behaviors. 6-DOF dynamics capture couplings and nonlinearities beyond simpler models.

Remark: Despite the complexity of 6-DOF models, the control architecture remains lightweight and scalable thanks to its decentralized structure. Each agent computes its control input using only local data. For real-time use, aerodynamic forces can be approximated with look-up tables or simplified models to maintain efficiency.

III. Proposed Cooperative Guidance Framework

We propose a control framework merging a potential-based formation approach and PNG to achieve simultaneous strikes. This ensures each missile orients correctly toward the target while maintaining collision-free spacing.

A. Proportional Navigation Guidance (PNG)

PNG is a widely used approach for single-missile engagement. Let

$$\mathbf{r}_{\text{LOS}}^{(i)}(t) = \mathbf{p}_t^{e,(i)}(t) - \mathbf{p}_m^{e,(i)}(t) \tag{8}$$

be the line-of-sight (LOS) vector for missile i. In many applications, $\mathbf{p}_t^{e,(i)}$ is computed from local estimates of the target location, possibly incorporating neighbor positions:

$$\mathbf{p}_t^{e,(i)}(t) = \mathbf{p}_t^e + \mathbf{p}_m^{e,(i)}(t) - \frac{1}{|\mathcal{N}_i|} \sum_{j \in \mathcal{N}_i} \mathbf{p}_m^{e,(j)}(t). \tag{9}$$

This decentralized adjustment encourages alignment of the swarm's center with the nominal target.

LOS rotation rates $\dot{\lambda}_{xy}^{(i)}, \dot{\lambda}_{xz}^{(i)}$ relate to the missile's relative velocity. The PNG-induced guidance commands are:

$$a_{y,\text{guidance}}^{b,(i)}(t) = N_g V_p^{(i)}(t) \dot{\lambda}_{xy}^{(i)}(t), \tag{10}$$

$$a_{z,\text{guidance}}^{b,(i)}(t) = N_g V_p^{(i)}(t) \dot{\lambda}_{xz}^{(i)}(t), \tag{11}$$

where N_g is the navigation constant, commonly around 3–5, and $V_p^{(i)}$ is the speed of missile i.

B. Formation Control via Potential Functions

Simultaneous arrival also demands cohesion and safety. We adopt a formation control law combining a velocity damping term and attraction-repulsion potentials [19]. For missile i,

$$\mathbf{a}_{\text{form}}^{e,(i)}(t) = -k_{\text{vel}}\big(\mathbf{v}_m^{e,(i)}(t) - \mathbf{v}_{\text{impact}}^{e,(i)}(t)\big) + \sum_{j\in\mathcal{N}_i} g(\mathbf{p}_m^{e,(i)}(t) - \mathbf{p}_m^{e,(j)}(t)), \tag{12}$$

where $k_{\text{vel}} > 0$ is a tuning gain, and $\mathbf{v}_{\text{impact}}^{e,(i)}$ is a reference velocity guiding the swarm toward synchronized impact times. $g(\cdot)$ defines spacing via attraction–repulsion.

A convenient choice for $\mathbf{v}_{\text{impact}}^{e,(i)}$ uses the local estimate of time-to-go $t_{\text{go}}^{(i)}$:

$$\mathbf{v}_{\text{impact}}^{e,(i)}(t) = \frac{\mathbf{r}_{\text{LOS}}^{(i)}(t)}{t_{\text{go}}^{(i)}}, \quad \|\mathbf{v}_{\text{impact}}^{e,(i)}(t)\| \le v_{\max}, \tag{13}$$

where $t_{\text{go}}^{(i)}$ can be computed via range-over-closure-rate estimates, or consensus-based approaches [4].

Finally, convert $\mathbf{a}_{\text{form}}^{e,(i)}(t)$ to the missile's body frame by a suitable rotation matrix $T_{b/e}^{(i)}(t)$:

$$\mathbf{a}_{\text{form}}^{b,(i)}(t) = T_{b/e}^{(i)}(t)\,\mathbf{a}_{\text{form}}^{e,(i)}(t).$$

C. Combined Control Law

To merge formation and guidance objectives, the net body-frame accelerations for missile i become:

$$a_x^{b,(i)}(t) = k_t a_{\text{form},x}^{b,(i)}(t) + g_x^{b,(i)}(t), \tag{14}$$

$$a_y^{b,(i)}(t) = W_f a_{\text{form},y}^{b,(i)}(t) + W_t a_{y,\text{guidance}}^{b,(i)}(t) + g_y^{b,(i)}(t), \tag{15}$$

$$a_z^{b,(i)}(t) = W_f a_{\text{form},z}^{b,(i)}(t) + W_t a_{z,\text{guidance}}^{b,(i)}(t) + g_z^{b,(i)}(t), \tag{16}$$

where $g_x^{b,(i)}, g_y^{b,(i)}, g_z^{b,(i)}$ account for gravity compensation in body coordinates. k_t, W_f, W_t are weighting parameters for formation and PNG terms. While tuning these parameters can be done systematically, we rely on manual selection for illustration.

IV. Lyapunov-Based Stability Analysis

In this section, we decompose the problem into three key components: **Formation Potential**, **Velocity Mismatch**, **Target Error**, each addressed by a dedicated Lyapunov term. By combining these terms into a single composite Lyapunov function (or using interconnected lemmas), we demonstrate that the proposed guidance strategy achieves stable, collision-free formations, velocity synchronization, and convergence to the target plane at a common final time.

A. Assumptions

The stability analysis relies on three assumptions: (1) reference velocities vary slowly over time, i.e., $\|\dot{\mathbf{v}}_{\text{impact}}^{e,(i)}(t)\| \le \epsilon$ with $\epsilon \ll k_{\text{vel}}$; (2) the target is either static or its velocity is negligible ($\mathbf{v}_t^e \approx 0$). This assumption can be relaxed to include bounded target velocities by modifying the PNG term accordingly, which remains a topic for future work involving dynamic or evasive targets; and (3) the communication graph $\mathcal{G}$ is undirected, ensuring bidirectional data exchange.

B. Lyapunov Components

We define three partial Lyapunov functions:

(i) Formation Potential:

$$V_{\text{form}}(t) = \sum_{i<j} U\big(\|\mathbf{p}_m^{e,(i)}(t) - \mathbf{p}_m^{e,(j)}(t)\|\big), \tag{17}$$

where $U(\cdot)$ is large or infinite at small distances.

Lemma IV.1 (Formation Potential Decreasing)**.** *If the control law for missile i includes*

$$\sum_{j\in\mathcal{N}_i} g(\mathbf{p}_m^{e,(i)}(t) - \mathbf{p}_m^{e,(j)}(t)), \quad g(\mathbf{y}) = -\nabla U(\|\mathbf{y}\|),$$

then

$$\dot{V}_{form}(t) \;\le\; 0,$$

implying collision-free, stable inter-missile distances.

Proof. Because $\mathcal{G}$ is undirected, for every interaction $g(\mathbf{p}_m^{e,(i)}(t) - \mathbf{p}_m^{e,(j)}(t))$ there is a symmetric term $-g(\mathbf{p}_m^{e,(j)}(t) - \mathbf{p}_m^{e,(i)}(t))$, so the sum of pairwise interactions does not increase the potential. Detailed derivation can be found in [20]. □

(ii) Velocity Mismatch: To achieve synchronized arrival, each missile should follow a velocity profile $\mathbf{v}_{\text{impact}}(i)$. Define:

$$V_v = \frac{1}{2}\sum_{i=1}^{N} \|\mathbf{v}_m^{e,(i)}(t) - \mathbf{v}_{\text{impact}}^{e,(i)}(t)\|^2. \tag{18}$$

Lemma IV.2 (Velocity Mismatch Decreasing)**.** *Under the Assumption-1* we have

$$\dot{V}_v(t) \;\le\; 0. \tag{19}$$

Proof. Taking the derivative:

$$\dot{V}_v = \sum_{i=1}^{N} (\mathbf{v}_m^{e,(i)}(t) - \mathbf{v}_{\text{impact}}^{e,(i)}(t))^\top (\dot{\mathbf{v}}_m^{e,(i)}(t) - \dot{\mathbf{v}}_{\text{impact}}^{e,(i)}(t)). \tag{20}$$

From the control law:

$$\dot{\mathbf{v}}_m^{e,(i)}(t) = -k_{\text{vel}}(\mathbf{v}_m^{e,(i)}(t) - \mathbf{v}_{\text{impact}}^{e,(i)}(t)) + \epsilon. \tag{21}$$

where ϵ is assumed to be a small perturbation term resulting from other contributing factors and will be neglected for this calculation. Substituting:

$$\dot{V}_v = -k_{\text{vel}} \sum_{i=1}^{N} \|\mathbf{v}_m^{e,(i)}(t) - \mathbf{v}_{\text{impact}}^{e,(i)}(t)\|^2 + \sum_{i=1}^{N} (\mathbf{v}_m^{e,(i)}(t) - \mathbf{v}_{\text{impact}}^{e,(i)}(t))^\top \dot{\mathbf{v}}_{\text{impact}}^{e,(i)}(t). \tag{22}$$

By Assumption 1 ($\|\dot{\mathbf{v}}_{\text{impact}}^{e,(i)}(t)\|$ is small), the last term is small. Hence,

$$\dot{V}_v \le -k_{\text{vel}} V_v. \tag{23}$$

This guarantees exponential convergence of velocities to $\mathbf{v}_{\text{impact}}^{e,(i)}(t)$, leading to synchronized arrival. □

(iii) Target Error: For a theoretical derivation, let $\mathbf{v}_t^e \approx 0$ or be bounded, in line with Assumption-2. Then define:

$$V_{\text{target}}(t) = \sum_{i=1}^{N} \|\mathbf{p}_m^{e,(i)}(t) - \mathbf{p}_t^{e,(i)}(t)\|^2. \tag{24}$$

We adopt a simplified PNG acceleration:

$$\mathbf{a}_{\text{PNG}}^{(i)} = -\,k_{\text{target}}\big(\mathbf{p}_m^{e,(i)}(t) - \mathbf{p}_t^{e,(i)}(t)\big). \tag{25}$$

Lemma IV.3 (Target Error Decreasing)**.** With the above PNG law and $\mathbf{v}_t^e \approx \mathbf{0}$, one obtains

$$\dot{V}_{target}(t) \;\le\; -\,\beta\, V_{target}(t), \quad \beta = 2\,k_{target} > 0. \tag{26}$$

Thus each missile's position converges exponentially to $\mathbf{p}_t^e$.

Proof. Differentiate $V_{\text{target}} = \sum_i \|\mathbf{p}_m^{e,(i)}(t) - \mathbf{p}_t^{e,(i)}(t)\|^2$. If $\mathbf{v}_m^{e,(i)}(t)$ aligns with $-(\mathbf{p}_m^{e,(i)}(t) - \mathbf{p}_t^{e,(i)}(t))$ under the simplified PNG acceleration, then

$$\begin{aligned}\dot{V}_{\text{target}} &\approx \sum_{i=1}^{N} 2(\mathbf{p}_m^{e,(i)}(t) - \mathbf{p}_t^{e,(i)}(t))^{\mathsf{T}}\mathbf{v}_m^{e,(i)}(t) \\ &\approx\; -2\,k_{\text{target}} \sum_{i=1}^{N} \|\mathbf{p}_m^{e,(i)}(t) - \mathbf{p}_t^{e,(i)}(t)\|^2, \end{aligned} \tag{27}$$

implying $\dot{V}_{\text{target}} \le -\,\beta\, V_{\text{target}}$ with $\beta > 0$. □

C. Main Theorem: Collision-Free, Time-Synchronized, Target Convergence

Combining these partial functions into a composite Lyapunov function:

$$V_{\text{combined}}(t) = V_{\text{form}}(t) + \alpha\, V_v(t) + \kappa\, V_{\text{target}}(t), \quad \alpha, \kappa > 0, \tag{28}$$

we obtain:

Theorem IV.4 (Swarm Guidance: Combined Stability)**.** Suppose:

1) $V_{\text{form}}(t)$ is nonincreasing via potential-based inter-missile control (Lemma IV.1).
2) $V_v(t)$ is nonincreasing via velocity damping and slow $\mathbf{v}_{\text{impact}}^{(i)}$ updates (Lemma IV.2).
3) $V_{\text{target}}(t)$ also decreases under simplified PNG, ensuring each missile converges to $\mathbf{p}_t^e$ (Lemma IV.3).

Then the swarm remains collision-free, synchronizes velocities to meet the same final time, and converges onto the target region $\mathcal{P}$.

Proof. Define a single Lyapunov-like function:

$$V_{\text{combined}}(t) = V_{\text{form}}(t) + \alpha\, V_v(t) + \kappa\, V_{\text{target}}(t), \tag{29}$$

for some positive gains $\alpha, \kappa > 0$. By Lemmas IV.1-IV.3, each individual derivative satisfies

$$\dot{V}_{\text{form}}(t) \;\le\; 0, \quad \dot{V}_v(t) \;\le\; 0, \quad \dot{V}_{\text{target}}(t) \;\le\; 0. \tag{30}$$

Bounding Cross Terms. In practice, each derivative may contain cross terms that couple, e.g., potential-based forces with velocity damping. Let us sketch how these are bounded:

- $\mathbf{a}_{\text{form}}^{(i)}$ includes a $-k_{\text{vel}}(\mathbf{v}_m^{(i)} - \mathbf{v}_{\text{impact}}^{(i)})$ term plus potential-based terms $g(\mathbf{p}_m^{(i)} - \mathbf{p}_m^{(j)})$.
- For V_v, cross terms arise such as

$$(\mathbf{v}_m^{(i)} - \mathbf{v}_{\text{impact}}^{(i)})^{\mathsf{T}} \sum_{j \in \mathcal{N}_i} g(\dots), \tag{31}$$

which we can bound via Cauchy–Schwarz,

$$\big|(\mathbf{v}_m^{(i)} - \mathbf{v}_{\text{impact}}^{(i)})^{\mathsf{T}} \sum_j g(\dots)\big| \;\le\; \|\mathbf{v}_m^{(i)} - \mathbf{v}_{\text{impact}}^{(i)}\|\, \|\sum_j g(\dots)\|. \tag{32}$$

If the potential gradient ∇U is bounded (due to finite initial dispersion), then $\big\|\sum_j g(\dots)\big\| \le G_{\max}$. Summing over i yields a bound linear in $\|\mathbf{v}_m^{(i)} - \mathbf{v}_{\text{impact}}^{(i)}\|$.

- Similarly, for target-error coupling, $\mathbf{a}_{\text{PNG}}^{(i)}$ might also cause cross terms. But as long as the negative damping in $-k_{\text{vel}}\|\dots\|^2$ is large enough to dominate linear bounding terms, the net effect remains ≤ 0.

Hence, by selecting the gains α, κ, and k_{vel} sufficiently large, one ensures that any positive cross contribution is overshadowed by the negative main terms. Thus we obtain

$$\dot{V}_{\text{combined}}(t) \;\le\; 0. \tag{33}$$

□

V. Simulation Setup and Results

We validate the framework in MATLAB/Simulink with $N = 5$ missiles. Each missile is governed by 6-DOF equations and subject to aerodynamic forces and moments. The target region is a 2D polytopic set near $[6000, 6000, 12000]^T$. Missiles initially start dispersed around the origin.

A. Simulation Parameters

The swarm employs an attraction-repulsion term:

$$g_a(\|\mathbf{y}\|) = a, \tag{34}$$

$$g_r(\|\mathbf{y}\|) = b\, e^{-|\mathbf{y}|/c} + \frac{1}{(\|\mathbf{y}\| - d_{\min})^2 + \epsilon^2}, \tag{35}$$

The control response is influenced by the attraction-repulsion parameters a, b, and c in the inter-agent interaction function. A larger a strengthens the attraction toward neighbors, promoting tighter formations, while a higher b and a smaller c result in stronger repulsive forces via the exponential term. The corresponding values used in simulations are $a = 0.045$, $b = 2$, $c = 65$, $d_{\min} = 100$, and $\epsilon = 0.5$. Other control gains include $N_g = 3$, $k_{\text{vel}} = 1.5$, $W_f = 0.8$, $W_t = 0.2$, and $k_t = 0.33$. For the matrix $\mathbf{M}$ in the interaction function:

$$\mathbf{M} = \begin{bmatrix} 1 & 0 & 0 \\ 0 & 1 & 0 \\ 0 & 0 & 0 \end{bmatrix}, \quad \mathbf{H} = \begin{bmatrix} 1 & 0 & 0 \\ 0 & 1 & 0 \\ 0 & 0 & 1 \end{bmatrix}.$$

This configuration causes no repulsion along the z-axis, shaping the swarm primarily in the x-y plane while maintaining a cohesive layer in z.

B. Results and Analysis

Figures 1–2 illustrate a scenario where the missiles move in 3D and converge onto a target region defined in the xy-plane at $z = 12000$. The missiles arrive within a maximum temporal deviation ϵ_t of about 0.001 s in Table I, illustrating successful time synchronization. They sustain stable inter-agent distances above 100 units (Fig. 1) and exhibit negligible time-of-arrival differences (under 0.05 s). The angular approach to the target's normal vector (Fig. 2) confirms precise orientation in the final phases.

TABLE I
IMPACT-TIMES OF EACH MISSILE.

Missile	Impact Time
Missile-1	47.921
Missile-2	47.922
Missile-3	47.921
Missile-4	47.922
Missile-5	47.921

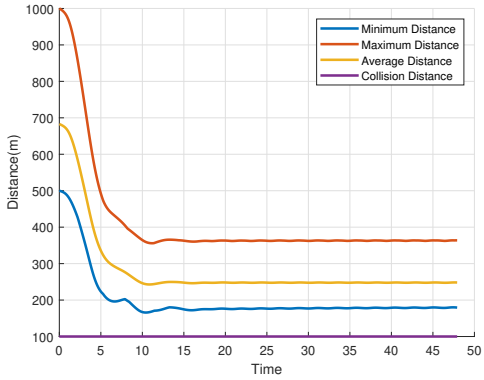

Fig. 1. Inter-missile distances remain above the safety threshold (100 m) throughout the engagement.

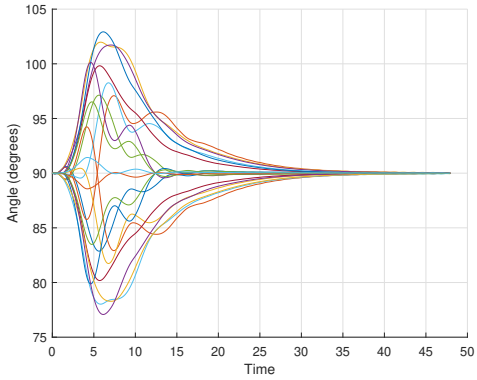

Fig. 2. Angle between missile position vectors and the region's normal vector, confirming correct orientation in final approach.

To illustrate flexibility, the matrix $\mathbf{M}$ can be altered:

$$\mathbf{M} = \begin{bmatrix} 0 & 0 & 0 \\ 0 & 1 & 0 \\ 0 & 0 & 1 \end{bmatrix},$$

exhibiting a similar behavior, but this time mapped onto a target region lying in the yz-plane. Figure 3 show the alignment angles in this alternative arrangement; simultaneous arrival and stable spacing are maintained. The missiles arrive within a maximum temporal deviation ϵ_t of about 0.008 s in Table II.

TABLE II
IMPACT-TIMES OF EACH MISSILE.

Missile	Impact Time
Missile-1	47.89
Missile-2	47.89
Missile-3	47.898
Missile-4	47.896
Missile-5	47.89

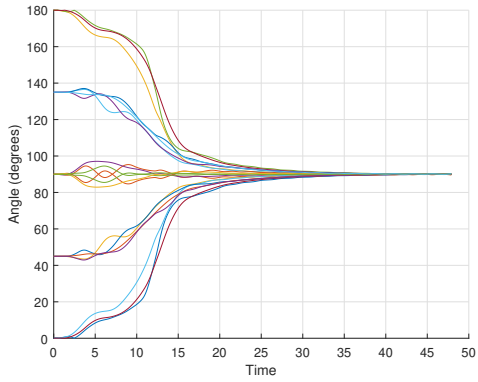

Fig. 3. Angular convergence to the target region's normal in the modified $\mathbf{M}$ scenario.

And finally to investigate **scalability**, the swarm size is increased to ten missiles. In this scenario attraction gain a and repulsion gain c are reduced to 0.025 and 57.0 respectively

TABLE III
IMPACT-TIMES OF EACH MISSILE.

Missile-1	48.18	Missile-2	48.183
Missile-3	48.183	Missile-4	48.182
Missile-5	48.18	Missile-6	48.183
Missile-7	48.183	Missile-8	48.183
Missile-9	48.18	Missile-10	48.183

The time synchronization remains robust, with $\epsilon_t \leq 0.003$ s despite the larger number of missiles Table III. Figure 4 shows that all missiles converge to the polytopic reigon. Although results with 10 missiles show strong synchronization, scalability to larger swarms (e.g., $N > 20$) may require bounding interaction ranges or using hierarchical consensus structures to maintain computational feasibility.

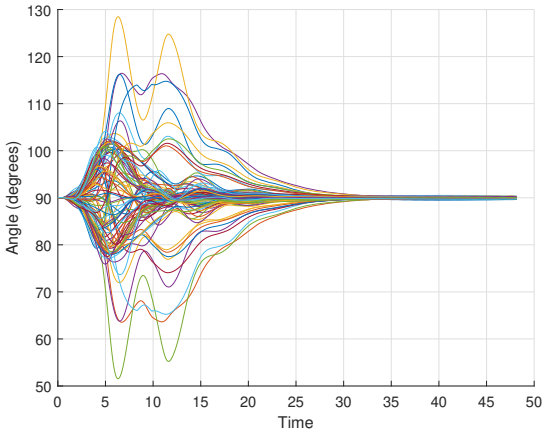

Fig. 4. Angular convergence to the target region's normal in the 10 missiles scenario

Overall, the simulations indicate that the combined approach successfully merges collision-free formation control, realistic missile dynamics, and precise terminal guidance. The swarm consistently reaches the target plane in a synchronized manner, verifying the framework's practical relevance and theoretical stability. These results show decentralized guidance is scalable and robust for coordinated strikes, where precision timing and spatial alignment are critical operational goals.

VI. Concluding Remarks

We introduced a cooperative guidance framework that unifies potential-based formation control and PNG for swarms of 6-DOF missiles targeting a 2D polytopic region in 3D space. A key innovation is the decentralized mechanism where each missile's local estimate of the target location is adjusted according to its neighbors, leading to alignment of the swarm's collective center and facilitating synchronous strikes. The 6-DOF model captures realistic aerodynamic and thrust effects, and the Lyapunov analysis clarifies how inter-agent potentials, velocity damping, and target convergence interact to maintain overall stability and collision avoidance.

Limitations: This work assumes static or slowly-varying targets, ideal communication links, and homogeneous agent models. Extension to dynamic or adversarial settings is reserved for future work.

Future work may focus on extending the framework to handle dynamic and maneuvering targets with unpredictable motion, as well as addressing communication constraints such as delays, packet losses, and bandwidth limits. Another direction includes integrating machine learning methods—such as reinforcement learning or evolutionary optimization—to improve adaptability and parameter tuning. Lastly, investigating implementation feasibility, including computational efficiency, parameter sensitivity (e.g., N_g, k_{vel}, W_f, W_t), and robustness against sensor noise, will be crucial for real-world deployment.

References

[1] Y. Chen, J. Wang, J. Shan, and M. Xin, "Cooperative guidance for multiple powered missiles with constrained impact and bounded speed," *Journal of Guidance, Control, and Dynamics*, vol. 44, pp. 1–17, 01 2021.

[2] E. Zhao, S. Wang, T. Chao, and M. Yang, "Multiple missiles cooperative guidance based on leader-follower strategy," in *Proceedings of 2014 IEEE Chinese Guidance, Navigation and Control Conference*, 2014, pp. 1163–1167.

[3] M. Xiaomin, D. Yang, L. Xing, and W. Sentang, "Behavior-based formation control of multi-missiles," in *2009 Chinese Control and Decision Conference*, 2009, pp. 5019–5023.

[4] I.-S. Jeon, J.-I. Lee, and M.-J. Tahk, "Impact-time-control guidance law for anti-ship missiles," *IEEE Transactions on Control Systems Technology*, vol. 14, no. 2, pp. 260–266, 2006.

[5] J. Meng, Z. Yang, J. Huang, H. Piao, Y. Zhao, and D. Zhou, "Three-dimensional multi-missile cooperative guidance law with time and space constraints," in *2022 22nd International Conference on Control, Automation and Systems (ICCAS)*, 2022, pp. 931–937.

[6] Q. Zhao, X. Dong, X. Song, and Z. Ren, "Time-varying formation pursuit based cooperative guidance for multiple missiles to intercept a maneuvering target," in *2018 37th Chinese Control Conference (CCC)*, 2018, pp. 4779–4784.

[7] Y.-Y. An, K.-K. Park, and C.-K. Ryoo, "A study of close-formation approach attack tactics of multiple anti-ship missiles," in *2018 9th International Conference on Mechanical and Aerospace Engineering (ICMAE)*, 2018, pp. 362–365.

[8] J. Zhou, Y. Lv, G. Wen, X. Wu, and M. Cai, "Three-dimensional cooperative guidance law design for simultaneous attack with multiple missiles against a maneuvering target," in *2018 IEEE CSAA Guidance, Navigation and Control Conference (CGNCC)*, 2018, pp. 1–6.

[9] J. Song, S. Song, and S. Xu, "Three-dimensional cooperative guidance law for multiple missiles with finite-time convergence," *Aerospace Science and Technology*, vol. 67, pp. 193–205, 2017. [Online]. Available: https://www.sciencedirect.com/science/article/pii/S1270963816308136

[10] W. Zhang, B. Lu, and Q. Xia, "Finite time convergence cooperative guidance law for non-maneuvering moving targets," in *2019 IEEE International Conference on Unmanned Systems (ICUS)*, 2019, pp. 7–12.

[11] H. Chen and Y. Nan, "Three-dimensional interception guidance law for cooperative aircraft in finite time based on non-singular sliding mode control," in *2021 33rd Chinese Control and Decision Conference (CCDC)*, 2021, pp. 5267–5272.

[12] P. Wu, J. Huang, X. Li, and B. Chen, "Multi-missile routes co-planning method based on improved ant colony algorithm," in *2023 42nd Chinese Control Conference (CCC)*, 2023, pp. 5750–5755.

[13] J. Hou, X. Ji, Z. Liu, and L. Gao, "Distributed multi-missile salvo attack," in *Proceedings of the 33rd Chinese Control Conference*, 2014, pp. 887–890.

[14] L. Chen, J. Shen, W. Wang, H. Peng, and K. Liu, "Distributed cooperative guidance for simultaneous arrival without numerical singularities," in *2024 43rd Chinese Control Conference (CCC)*, 2024, pp. 3851–3856.

[15] Q. Xu, J. Ge, and T. Yang, "Multiple missiles cooperative guidance based on proportional navigation guidance," in *2020 Chinese Control And Decision Conference (CCDC)*, 2020, pp. 4423–4430.

[16] C. Luo, C. Zhou, and X. Bu, "Multi-missile phased cooperative interception strategy for high-speed and highly maneuverable targets," *IEEE Transactions on Aerospace and Electronic Systems*, pp. 1–28, 2024.

[17] R. Olfati-Saber and R. Murray, "Consensus problems in networks of agents with switching topology and time-delays," *IEEE Transactions on Automatic Control*, vol. 49, no. 9, pp. 1520–1533, 2004.

[18] G. M. Siouris, *Missile Guidance and Control Systems*. New York, NY, USA: Springer, 2004.

[19] G. Fedele, L. D'Alfonso, and V. Gazi, "A generalized gazi–passino model with coordinate-coupling matrices for swarm formation with rotation behavior," *IEEE Transactions on Control of Network Systems*, vol. 9, no. 3, pp. 1227–1237, 2022.

[20] V. Gazi and K. M. Passino, *Swarm Stability and Optimization*. Springer Verlag, January 2011.